Investigation of the effect of mineralogy as rate-limiting factors in large particle leaching

*Yousef Ghorbani[1, 2], Megan Becker[1], Jochen Petersen[1, 2], Aubrey, N. Mainza[1] and Jean-Paul Franzidis[1]

[1]Minerals to Metals Signature Theme, Department of Chemical Engineering, University of Cape Town, Private Bag X6, Rondebosch 7701, South Africa. (*Corresponding author: yousef.ghorbani@uct.ac.za)

[2] Centre for Bioprocess Engineering Research (CeBER) Department of Chemical Engineering, University of Cape Town

Abstract

Although heap leaching is by now well established in the mining industry, the process remains limited by low recoveries with different rate-limiting factors that are not clearly understood. In this study, three large particle size classes (+19/-25, +9.5/-16, +4.75/-5 mm) were prepared from a sphalerite ore by two different methods of comminution (HPGR and cone crusher). The particles were then packed into leach reactors that were operated continuously for eleven months with well-mixed internal circulation of the leach solution. Characterization of the residue of the leach reactors indicated that there are areas within the ore particles where although sphalerite grains are accessible to the solution, they remain unreacted. X-ray tomography and QEMSCAN® analysis of the selected samples before, during and after leaching, showed increased leaching of sphalerite grains associated with pyrite due to galvanic interactions. Mineral chemistry (Fe, Mn content of sphalerite) and jarosite precipitation were also investigated as factors influencing sphalerite leaching.

Key words: mineral composition, sphalerite, X-ray tomography, mineral association, heap leaching.

INTRODUCTION

Although heap leaching is by now well established in the mining industry, the process remains limited by low recoveries (up to 60-70 %), long extraction times (over a 1-2 year period), and high operating costs, especially in terms of acid consumption. As the technology becomes more and more adopted, it is increasingly clear that the successful application of heap leaching technology will ultimately depend on having a comprehensive understanding of the underlying fundamental processes for optimisation to take place (Acevedo, 2002; Dreisinger, 2006; Mellado *et al*., 2009).

Ores are placed in heaps in a relatively coarse particle size distribution, reaching up to 25 mm top size for crushed and agglomerated ores and as much as 500 mm for ROM ores in dump leaching (Watling, 2006). Leaching from large ore particles is, however, poorly understood and commonly assumed to follow shrinking core type behaviour. A conventional shrinking core approach would work only for gangue particles that are homogeneously porous and have mineral grains well distributed throughout (Liddell, 2005; Veglio et al., 2001). In fact, there is a dearth of literature sources that offer any evidence for the validity of this assumption in the given context (Ghorbani et al., 2011a). Recent experimental evidence suggests that leaching from large particles occurs only at the surface and in subsurface regions, which are accessible from the surface by cracks and pores (Malmström et al., 2008; Sracek et al., 2006; Strömberg and Banwart, 1999; Ghorbani et al., 2011b). This would suggest that leaching behaviour might be closely related to the method by which the ore has been crushed prior to leaching (Rawlings, 1999; Rawlings et al., 2005; Watling, 2006).

The relatively coarse particle size distribution is one of the unique features of heaps that poses a major technical challenge; namely to suitably expose the mineral grains within the ore to the lixiviant, be it acid, ferric ions or bacteria and oxygen. One possible approach to improving recovery in the heap is to introduce fractures into large ore particles, so increasing the surface area available for lixiviant attack. Extensive cracking can be induced in a number of ways; one of which is through compression or particle bed breakage with the High-pressure grinding rolls (HPGR).

This paper forms part of a larger study aimed at understanding the mechanisms taking place during large particle leaching that has been conducted on a sphalerite ore. The initial ore sample was prepared using cone crusher and HPGR. Comminution results are reported in (Ghorbani et al., 2011c). Initial particle characterisation using mineralogy and x-ray computed tomography (X-ray CT) consistently identified the prevalence of micro-cracks and higher porosity for particles prepared by compression breakage (HPGR) as compared to conventional crushing by impact breakage (Ghorbani et al., 2011d). In this study, three large particle size classes (+23/-25, +14/-16, +5.25/-6.75 mm) were

prepared from a sphalerite ore from the Northern Cape, South Africa, by two different methods of comminution (HPGR and cone crusher) and packed into leach reactors, which were operated continuously and well mixed through internal circulation of the leach solution for 11 months.

A comparison of the effect of the different comminution devices on metal extraction indicated that HPGR crushed ore leached more rapidly in all particle size classes and showed 10 to 15% additional zinc leach extraction (Figure 1), since the presence of micro-cracks provides an additional surface-front of target mineral grains for attack by the leaching solution, and a higher prevalence of attachment sites for microorganisms for regeneration of ferrous to ferric iron as leach reagent (Ghorbani et al., 2011e).

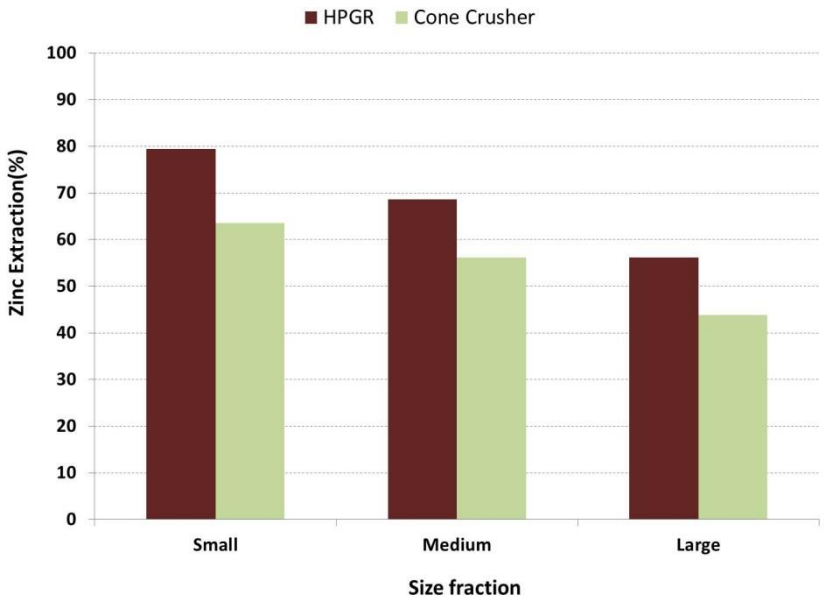

Figure 1: Leachability of zinc for different particle size classes, HPGR-95 bar product versus cone crusher.

Characterization of the residue of the leach reactors indicated that there are areas within the ore particles where although sphalerite grains are accessible to the solution, they remain unreacted. These results indicate that although accessibility to the reagent is necessary, a variety of other rate-limiting factors in large particle leaching can hamper or prevent leaching of an ore.

The objective of this study is to investigate the role of mineralogy as a rate-limiting factor in large particle leaching. This is done using 3D particle characterisation from X-ray CT in combination with detailed 2D mineralogical characterisation (QESCAN, EMPA, SEM/EDS). The focus areas in this study

are the effect of mineral chemistry and impurity content, mineral association and mineral precipitation on the rate of sphalerite leaching.

EXPERIMENTAL

Sample Preparation

A bulk sample of sphalerite ore was obtained from the Gamsberg Zinc mine in the Northern Cape Province, South Africa. The sample, after primary crushing by jaw crusher, was split and prepared into 250 kg bags for further crushing by either HPGR or cone crusher at Mintek in Randburg, South Africa. HPGR test work was conducted using a Köppern unit equipped with 1 m diameter rolls and was fully instrumented to control and record hydraulic and nitrogen pressures and throughput. The unit was fitted with profiled hexadur. Further details of comminution in terms of HPGR pressure settings, energy and particles size distribution (PSD) are given in Ghorbani et al., 2012c. The same top size was fed to the cone crusher and crushed down to -25 mm. Products from the cone crusher and HPGR were then screened into five size fractions (+23/-25, +16/-23, +14/-16, +6.75/-14, +5.25/-6.75 mm). In this study, subsamples from the (+19/-25), +9.5/-16, +5.25/-6.75 mm) size fractions were used for the leach experiments.

Leach experiments

Selected sub-samples as summarised in Table 1 were packed into custom designed leach reactors in which the leach solution was continuously circulated around stacked baskets containing ore particles. The particles were fully immersed in leach solution and the reactor was operated in continuous mode for 11 months. Full details of reactor operation and chemical dynamics during leaching (pH, redox potential, Fe^{3+} and Fe^{2+} concentration as well as total Fe, Zn, Mg, Al and planktonic cell concentration) in the effluent solution are given in Ghorbani et al 2011e.

Table 1: Summary of the leach reactors.

Reactor	Crusher conditions	Size fraction (mm)	Zn Extraction (%)
A	HPGR-95 bar	Small size fraction (-6.75+5.25)	79.4
B	HPGR-95 bar	Medium size fraction (-16+14)	68.7
C	HPGR-95 bar	Large size fraction (-25+23)	59.1
D	HPGR-120 bar	Large size fraction (-25+23)	49.1
E	Cone Crusher	Small size fraction (-6.75+5.25)	63.5
F	Cone Crusher	Medium size fraction (-16+14)	56.1
J	Cone Crusher	Large size fraction (-25+23)	43.8
K	HPGR-45bar	Large size fraction (-25+23)	54.5

The reactors were stopped from time to time to investigate the progress of leaching by analysing X-ray CT images of individual tagged particles. After X-ray CT analysis, the tagged particles were returned to the reactors for leaching. A further sub-set of particles was also removed from the columns at each reactor stoppage to further validate the non-destructive X-ray CT analysis with those measurements obtained using more traditional, although destructive techniques such as SEM/EDS, QEMSCAN® and EMPA.

Mineralogical analysis

X-ray CT was used for 3-D characterization of the sphalerite particles prior to leaching, during the course of the leach experiments and after leaching. The non-destructive nature of this technique allowed a virtual “in-situ” characterisation of the ore particles during leaching. During the stoppage of the leach reactors, individual tagged particles (eight particles for small, four for medium and two for large size fraction) were analysed using X-ray CT.

Selected particles were washed using distilled water and dried to avoid the blocking of the cracks and microcracks with any precipitates that may have formed during the course of the leach experiments.

An HMXST CT scanner at X-Sight X-ray Services in Stellenbosch, South Africa, with 225 kV X-ray source, 3 µm resolution reflection target, and interchangeable Nano-tech 1 µm transmission target was used. The mineralogy of the measurements was calibrated using the dual energy method. The 3D volumes of the individual tagged particles were interrogated using the VG Studio Max software. Full details of the X-ray CT measurement conditions and data processing are summarised in Ghorbani et al., 2011 d.

QEMSCAN® was used to determine the bulk mineralogy of the ore sample (prior to and post leaching) as well as monitor the changes in mineralogy over the 11 month experiment. The QEMSCAN® unit used in this study was located at the University of Cape Town, and is based on a LEO SEM platform equipped with two Bruker 4010 SDD detectors. Operating conditions were set at 25 kV and 5 nÅ beam current. Measurements of the bulk mineralogy were obtained using the bulk mineralogical analysis (BMA) routine on a series of sized samples (+120; +90; +63; +38; -38) µm. Samples were dry sized to avoid the dissolution of any soluble precipitates that may have formed during the course of the leach experiments. Individual ore particles (5 to 25 mm) that were sampled at each of the reactor stoppages were analysed using the Field Image analysis routine. Ore samples were mounted in epoxy resin and prepared into polished 30 mm diameter mounts. Pixel spacing between 3 and 5 µm was used for BMA analysis (depending on the size fraction) and a pixel spacing of 20 µm was used for the field image analysis. The results from QEMSCAN® were validated by comparison with XRF data and QXRD data.

Quantitative X-ray diffraction was used to determine the amount of the different major mineral phases. Samples were analysed using a Bruker D8 advance laboratory X-Ray Diffractometer equipped with a CoK_{α} as a radiation source (λ= 1.78897 Å) and a position sensitive detector (Bruker Vantec), operating at 35 kV and 40 mA with Bragg Brentano geometry. Samples were prepared for analysis using a McCrone micronizing mill. Phase quantification was performed using the Bruker Topas Rietveld refinement software.

The chemical assays were determined using wavelength dispersive X-ray Fluorescence spectrometry. Selected samples were prepared into fusion discs for major element analysis on a Philips PW1480 wavelength dispersive XRF spectrometer with a dual target Mo/Sc x-ray tube. All measurements are made with the tube at 50 kV, 50 mA. Intensity data are collected using the Philips X40 software. All peaks are corrected for background. Matrix corrections are made on all elements using the de Jongh model in the X40 software. Theoretical alpha coefficients calculated using the Philips on-line ALPHAS programme, are used in the de Jongh model.

Selected samples of the feed and residue of the reactors were analysed by EMPA to determine sphalerite composition (mineral chemistry) and the amount of impurities. Elemental mapping was also used for 2D characterization of unreacted sphalerite within the residue of the reactors. Microprobe analysis of the samples was performed at the University of Cape Town using a Jeol JXA 8100 electron microprobe, equipped with four wavelength-dispersive spectrometers. Operating conditions for quantitative analysis were set at 25 kV and 20 nÅ with counting times set on 10s for peak and 5s for background (both upper and lower). Pyrite was used as a standard for Fe and S and the related metal standards were used for Zn, Mn and Cu for calibration. ZAF used as a matrix correction program. A pixel spacing of 1 µm was used for analysis elemental mapping. Preliminary investigations showed negligible Cd, and so this element was not included in the quantitative analysis. EMPA analyses were performed on the same blocks that were used for QEMSCAN® analysis.

SEM/EDS images of selected samples were taken to investigate the surface morphology of the particles, specifically to characterise any soluble minerals that may have precipitated during the course of the leach experiments. Images were obtained on a Nova Nano field emission gun (FEG) SEM at the University of Cape Town. The EDS spectra were collected with an Oxford Instruments X-MAX 20 mm^2 silicon drift detector (SDD) at beam energy of 20 keV.

RESULTS AND DISCUSSIONS

Mineral characterization

Bulk mineralogy

Major minerals identified by QEMSCAN® analysis of the feed sample included sphalerite (16.0 wt %) and pyrite (33.8 wt %) with lesser pyrrhotite, mica, kaolinite and quartz. Only very minor chalcopyrite and galena occurred, as well as alabandite and arsenopyrite (grouped as other sulfides). Quartz was the main silicate gangue mineral (25.5 wt. %). Table 2 shows the bulk mineralogical analysis of the feed.

Table 2: Bulk mineralogical composition of the ore sample as determined by QEMSCAN®.

Mineral	Amount (Wt. %)
Pyrrhotite	1.2
Pyrite	33.8
Sphalerite	16.0
Galena	0.2
Chalcopyrite	< 0.1
Other sulfides (mostly Molybdenite, Pentlandite, Arsenopyrite)	3.2
Garnet	0.3
K-Feldspar	0.4
Chlorite	1.7
Kaolinite	2.8
Phlogopite	7.9
Apatite	2.0
Calcite	< 0.1
Quartz	25.5
Fe oxides/hydroxides	1.9
Others	3.1

Mineral Chemistry

The crystal structure of sphalerite has long been recognised to accommodate a broad variety of elements, the most significant of which are Fe and Cd. Many elements enter the sphalerite structure via simple substitution of similar-sized ions ($Zn^{2+} \leftrightarrow Fe^{2+}$, Cd^{2+}, Mn^{2+}, Co^{2+} or $S^{2-} \leftrightarrow Se^{2-}$), or by coupled substitution (e.g., $Zn^{2+} \leftrightarrow Cu^{+}+In^{3+}$) (McClung and Viljoen, 2011).

Table 3 shows 30 individual spot analyses for impurity content of sphalerite sample as determined by as determined by EPMA. The composition of the sphalerite in this study is given in Table 4 and illustrates that the major impurities in sphalerite composition are Fe (9.72 ± 0.74 wt. %) and Mn (4.44 ± 1.10 wt. %). The average sphalerite composition is ($Zn_{0.78}$, $Mn_{0.07}Fe_{0.15}$) S, which is in agreement with McClung and Viljoen (2011). 2 of the 30 analyses of sphalerite with compositions at ~58-60 wt. % Zn are representative of another high Fe, Mn poor sphalerite population which was also described by McClung and Viljoen (2011). The results in this study are interpreted using the dominant sphalerite composition (Fe-Mn rich sphalerite).

Table 3: 30 individual spot analyses for impurity content of sphalerite sample as determined by EPMA (wt. %).

Sphalerite population	S	Cu	Fe	Zn	Mn
Fe and Mn rich (n=28)	33.81	0.00	10.55	51.38	4.83
	33.63	0.06	10.20	50.94	4.50
	33.99	0.01	9.53	51.59	4.87
	33.54	0.00	9.89	51.17	4.61
	33.87	0.00	10.35	51.93	4.67
	33.71	0.02	10.94	51.38	4.76
	34.34	0.01	10.01	50.90	4.85
	34.23	0.00	9.38	51.83	4.56
	34.01	0.00	9.60	51.93	4.40
	34.34	0.00	10.01	50.90	5.20
	34.34	0.01	9.98	51.57	4.85
	34.42	0.04	9.99	51.79	4.75
	34.25	0.01	9.34	53.86	3.54
	34.58	0.06	9.84	51.39	4.89
	34.56	0.00	9.25	52.07	4.06
	34.53	0.02	10.39	50.42	5.26
	34.41	0.00	9.91	51.40	5.10
	34.32	0.36	10.23	50.70	4.69
	34.07	0.05	9.63	51.90	4.91
	33.98	0.04	9.57	51.83	4.69
	34.46	0.03	9.78	51.70	4.96
	34.17	0.01	9.63	51.47	4.96
	34.11	0.00	9.54	51.97	4.86
	34.17	0.02	9.94	52.23	4.52
	33.80	0.02	9.60	51.82	4.99
	33.88	0.03	9.86	51.70	4.56
	33.89	0.03	9.97	51.22	5.01
	33.43	0.04	9.98	51.74	4.41
Fe rich (n=2)	33.32	0.04	7.57	58.43	0.64
	33.73	0.01	7.10	59.09	0.43

Table 4: Average of 30 individual spot analyses for impurity content of sphalerite sample as determined by EPMA (wt. %).

Element	S	Cu	Fe	Zn	Mn
Average	34.00	0.03	9.72	52.00	4.44
Standard deviation	0.34	0.06	0.74	1.88	1.10

Texture and mineral association

Mineral texture and association plays a key role in all mineral processing techniques including heap leaching. In heap leaching, mineral grains need not necessarily be liberated as free grains and only partial exposure of mineral grains may provide sufficient surface front for chemical attack by leaching solution. The sphalerite in this study can in general can be divided in two groups based on the grain size and association. The coarse sphalerite grains (≥ 5 mm) were associated with other base metal sulfides and the disseminated fine sphalerite grains (≤ 1 mm) showed a stronger associated to the gangue minerals. Unlike other Pb-Zn-Cu ores, e.g. the neighbouring Black Mountain / Broken Hill ores that are enriched in copper (Spry, and Petersen, 1989), sphalerite ore in this study does not show chalcopyrite disease, which is the intimate association of very fine chalcopyrite to sphalerite (Barton and Bethke, 1987). Sphalerite in this study can be further classified into six different classes based on the different comminution methods and their expected leaching behaviour (Figure 2):

a. Grains located at the surface of particles and exposed to the leach solution (e.g. grain marked A);
b. Grains located close to the surface of particles which become expose to the leach solutions only after other grains, have reacted (e.g. grain marked B);
c. Grains located inside the particles and not connected to the surface (e.g. grain marked C);
d. Grains located inside the particles but connected to the surface via pores or cracks (mostly in the particles crushed using HPGR) (e.g. grains marked D);
e. Grain with size bigger than 5 mm and could be liberated in the small size fraction (-6.75+5.25) mm and completely accessible for the leach solution (e.g. grains marked E);
f. Fine grains disseminated within the gangue mineral (mostly quartz that are completely inaccessible to the leach solution (e.g. grain marked F).

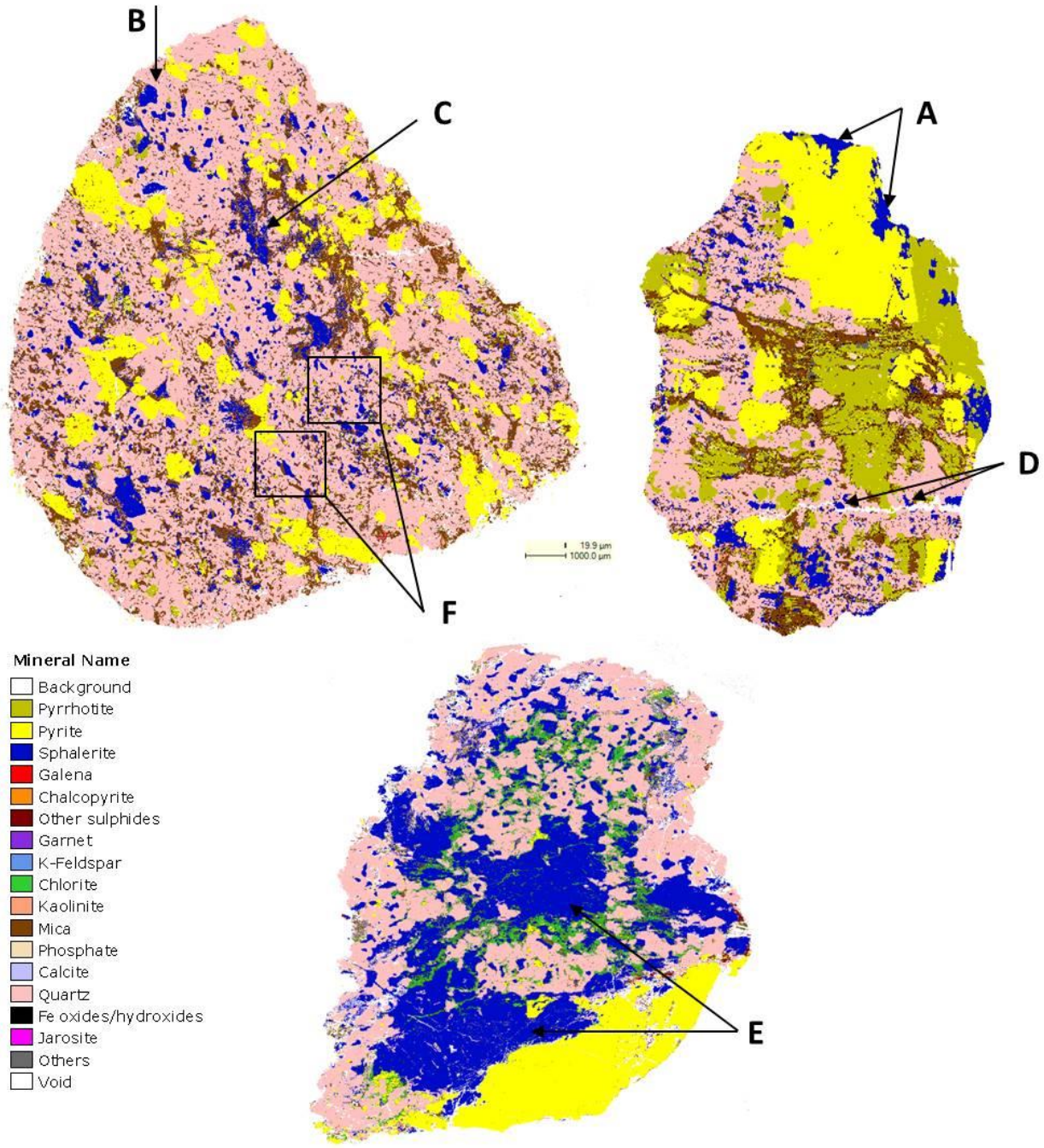

Figure 2: QEMSCAN® images of three ore particles illustrating six different classes of the sphalerite distribution (see the texture and mineral association section).

Effect of mineralogy on zinc extraction: Galvanic effects

Galvanic interactions between metal sulfide minerals are known to have a significant influence on chemical mineral processing methods such as flotation and hydrometallurgy (Ahonen and Tuovinen, 1995). In hydrometallurgy, galvanic interactions have been studied for several leaching and

bioleaching systems. In these systems, the galvanic interactions were shown to substantially increase the leaching of one or both of the minerals that constitute the galvanic cell, depending on the electrochemical characteristics of the minerals and on the occurrence of the distinct sulfides contained in the concentrates (Arce *et al*., 2002; Liu and Zhou, 2008; Urbano *et al*., 2007).

For semiconductive minerals, such as sulfides, direct contact of different minerals with dissimilar rest potentials initiates the galvanic effect. This effect has been modelled with galvanic cells through the redox reactions, where the mineral with the higher rest potential acts as the cathode, which is galvanically protected, while the mineral with the lower rest potential acts as an anode and its dissolution is favoured through electronic interactions. These interactions occur between sulfides, involving the flow of electrons from grains with a higher potential to grains with lower potentials, modifying the Fermi level of both minerals (Arce *et al*., 2002).

Galvanic interactions depend on the mineralogical association between the phases present in the ore sample. The presence of strong oxidizing ions, such as Fe^{3+}, present in solution results in enhanced corrosion current density of galvanic interaction between sulfides, with higher concentrations of strongly oxidizing ions leading to increased corrosion current density. Even if there is a large quantity of non-oxidizing and non-reducing ions, the corrosion current density will not significantly change (Cruz *et al*., 2005). The electrochemical behaviour of sulfide minerals is characterized by their rest-potential (Arce et al., 2002). The values vary depending on the origin of the mineral but the order generally remains consistent (Kocabag, 1985):

Pyrite > Chalcopyrite > Sphalerite > Pyrrhotite > Galena

To illustrate the importance of the order, consider two sulphides in contact in electrolyte. The sulfide with the lower rest-potential acts as the anode and undergoes oxidation by giving up electrons (Eq. (1)) to the sulfide with the higher rest-potential acting as the cathode. The Me in Eq. (1) stands for metal (e.g., zinc, copper, lead, etc.). The final electron acceptor is commonly oxygen, which is reduced to hydroxide (OH^-) (Eq. (2)). Another electron acceptor is ferric iron (Fe^{3+}), which is reduced to ferrous iron (Fe^{2+}) (Eq. (3)) (Rao and Finch, 1988; Ahonen and Tuovinen, 1995). This electrochemical process is known as galvanic interaction.

$$MeS \rightarrow Me^{2+} + S^{\circ} + 2e^{-} \qquad (1)$$

$$\frac{1}{2}O_2 + H_2O + 2e^{-} \rightarrow 2OH^{-} \qquad (2)$$

$$Fe^{3+} + e^{-} \rightarrow Fe^{3+} \quad (3)$$

Since pyrite is a dominant sulfide mineral in the Gamsberg ore (34 wt. %), the role of the pyrite on the leaching of sphalerite merits evaluation. The rest-potential of pyrite (0.66 V) is higher than that of sphalerite (0.46 V) (Kocabag, 1985) and, therefore, electrons flow from sphalerite, the anodic mineral, to pyrite, the cathodic mineral. As the anode, sphalerite is oxidized (Eq. (1)) and the cathodic reaction is either reduction of oxygen on the surface of pyrite (Eq. (2)) or reduction of ferric iron (Eq. (3)). This indicates that during bioleaching a galvanic current would flow from sphalerite to pyrite when they are in contact with one another. Figure 3 derived from the X-ray CT analysis, shows two areas of sphalerite associated with pyrite prior to leaching. After 6 months of treatment, the sphalerite has completely reacted. The sphalerite surface association to pyrite (i.e. % of the sphalerite grain perimeter) is illustrated in Figure 4 for the 8 different reactors prior to and after the leach experiment. The results show an overall decrease in the association of sphalerite to pyrite consistent with the selective oxidation of sphalerite relative to pyrite. The discrepancies in the data for reactors B and J are attributed to the statistical representativity of the coarse particles analysed. The QEMSCAN® particle images in Figure 5 similarly show a decrease in the association of sphalerite to pyrite during the course of the leach experiment. Note that sphalerite contained in the residue is completely associated with the gangue minerals.

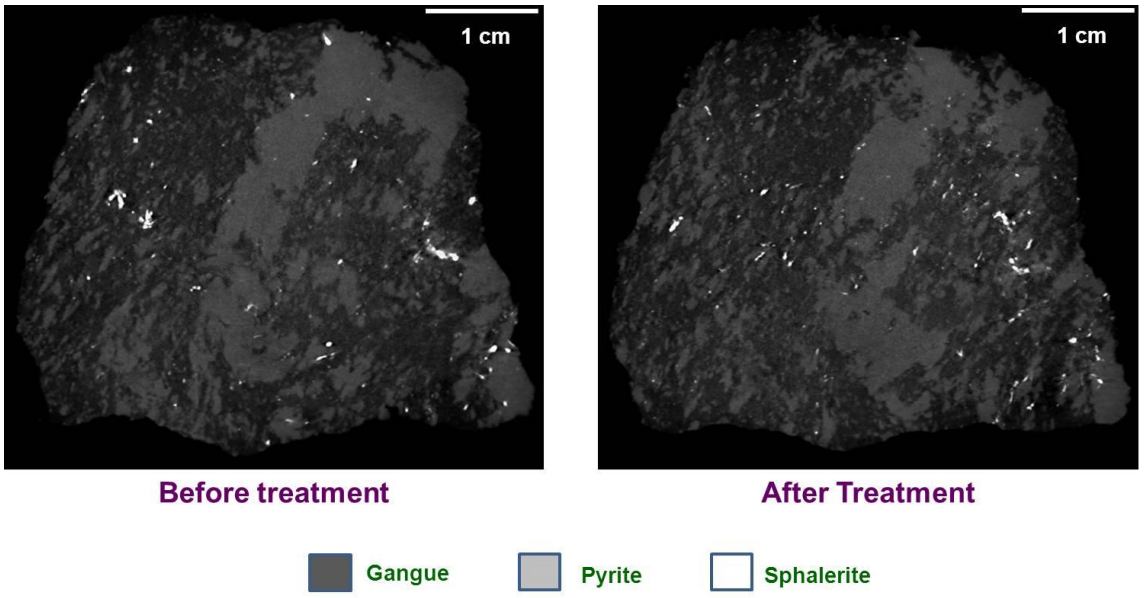

Figure 3: X-ray CT analysis results for the trend of depletion of the sphalerite association with pyrite in the ore particles before and after six months treatment.

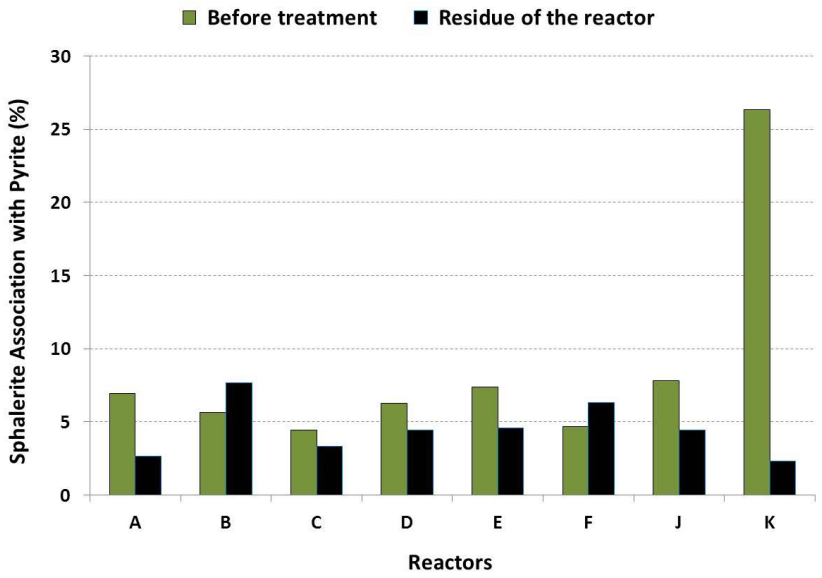

Figure 4: QEMSCAN® analysis results for the trend of the sphalerite association with pyrite in the leach reactors before and after leaching process.

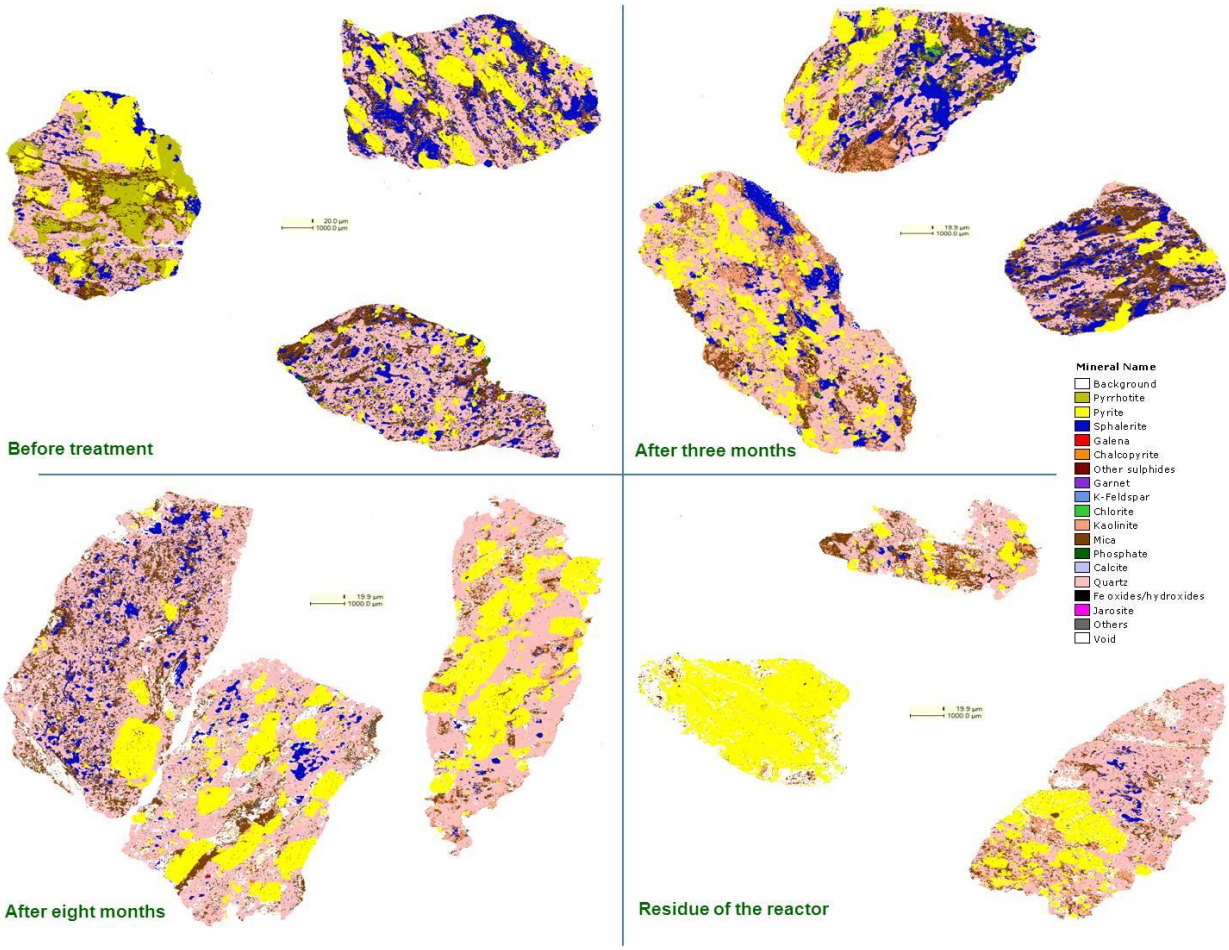

Figure 5: QEMSCAN® analysis results for the trend of depletion of the sphalerite association with pyrite in the ore particles before, during and after treatment.

Effect of mineralogy on zinc extraction: Association with gangue minerals

Characterization of the residue of the leach reactors indicated that most of the unreacted sphalerite grains occurred either as fine grains disseminated within the quartz (Figure 6a) or associated with mica (Figure 6b). As described in the sphalerite texture, fine grains disseminated within the gangue mineral (mostly quartz) are completely inaccessible to the leach solution. This indicates that diffusion of the reagent through the dense network of quartz to dissolve the disseminated fine sphalerite grains is practically impossible. For mica however, areas do exist where sphalerite is accessible to the solution, but the sphalerite grains still remain unreacted. Sphalerite grains associated with mica in the area shown in the Figure 6b are in the range of the penetration depth and theoretically must dissolve during the process. This suggests that some element of the association of sphalerite to mica is inhibiting the dissolution of sphalerite.

Mica is a common constituent of rocks, which during weathered forms secondary minerals such as vermiculite and interstratified mica/vermiculite, according to the environmental conditions. During weathering, mica minerals typically lose K from the interlayer positions and are transformed to expansible minerals such as vermiculite (Leonard and Sweed, 1970).

Dissolution and structural alteration of mica could be mediated by proton attack and bacterial oxidation of ferrous iron during the bioleaching process (Bigham et al., 2001). According to the results of the research by Bigham et al. (2001) and Bhatti et al. (2011), mica weathering was found to proceed via two pathways depending upon experimental conditions. At pH 2-3 in the presence of Fe^{3+}, K was preferentially stripped from the interlayer regions of phlogopite to form jarosite. Subsequent replacement of K by hydrated cations yielded expansible phases including vermiculite and interstratified vermiculite/phlogopite. Under these conditions, bacteria facilitated the weathering through the oxidation of Fe^{2+} to Fe^{3+}. At pH 1.5-2, the solubility product of jarosite was not exceeded, and preferential removal of K from the mica interlayer was diminished. Consequently, the formation of expansible layer silicate phases was halted and weathering proceeded by chemical dissolution mediated by proton attack of the mineral structure. It should be noted that the biological systems might also act as nutrient sinks and thereby enhance the structural alteration of mica through removal of interlayer K (Bhatti et al., 2012).

The formation of minor jarosite from the alteration of mica during the course of the 11 months of leaching would shield the surface of the sphalerite grains, thereby inhibiting sphalerite dissolution. Quantitative XRD confirmed the presence of minor jarosite during the leach experiment.

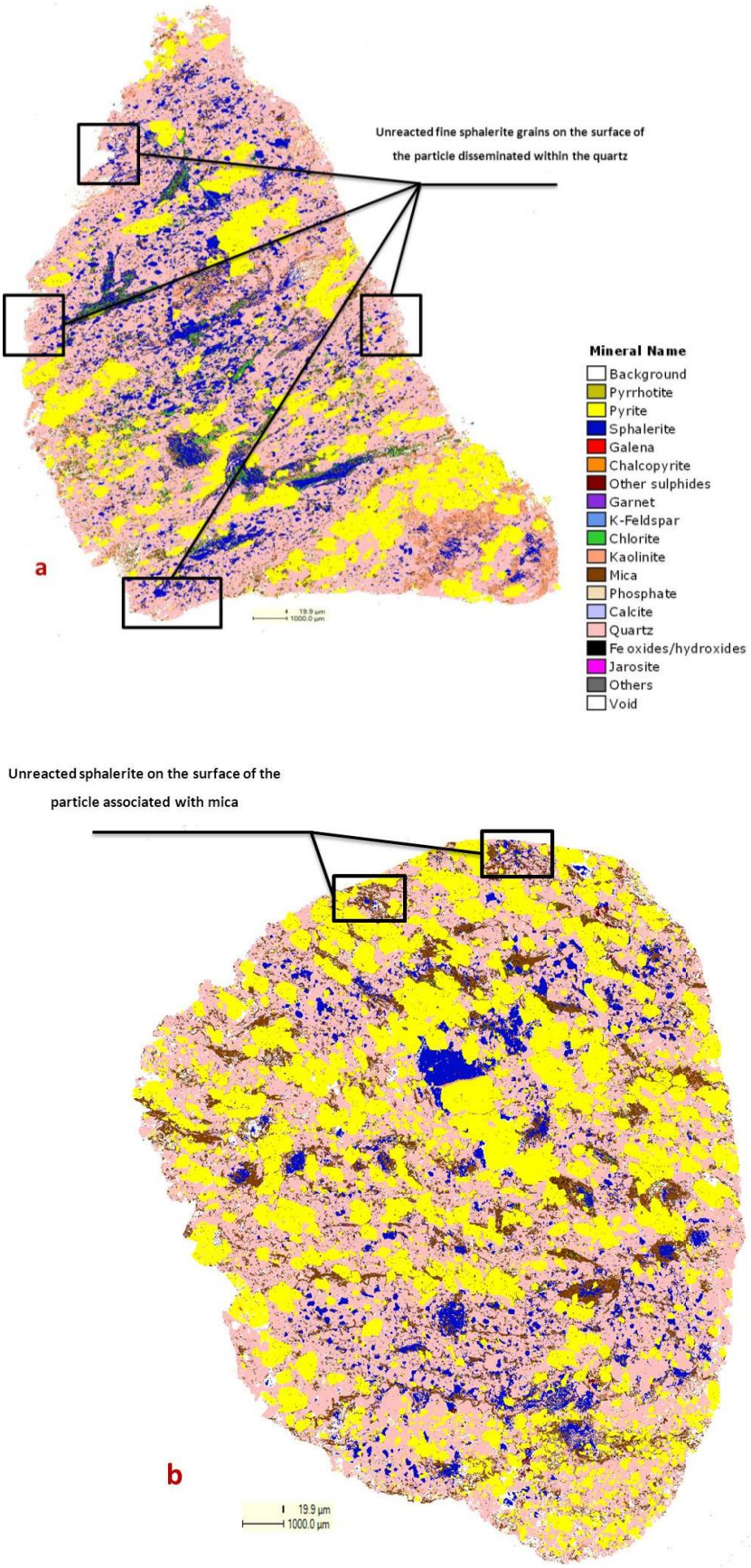

Figure 6: Unreacted sphalerite grains, fine grains disseminated within the quartz (a), associated with mica (b).

The sphalerite surface association to mica and quartz (i.e. % of the sphalerite grain perimeter) is illustrated in Figures 7 for the eight different reactors prior to and after the leach experiment. The results show an overall increase in the association of sphalerite to Mica and quartz. This indicates that sphalerite grains association to mica and quartz remain unreacted and there is a preferential leaching of sphalerite grains associated with pyrite. The discrepancies in the data are attributed to the statistical representativity of the coarse particles analysed.

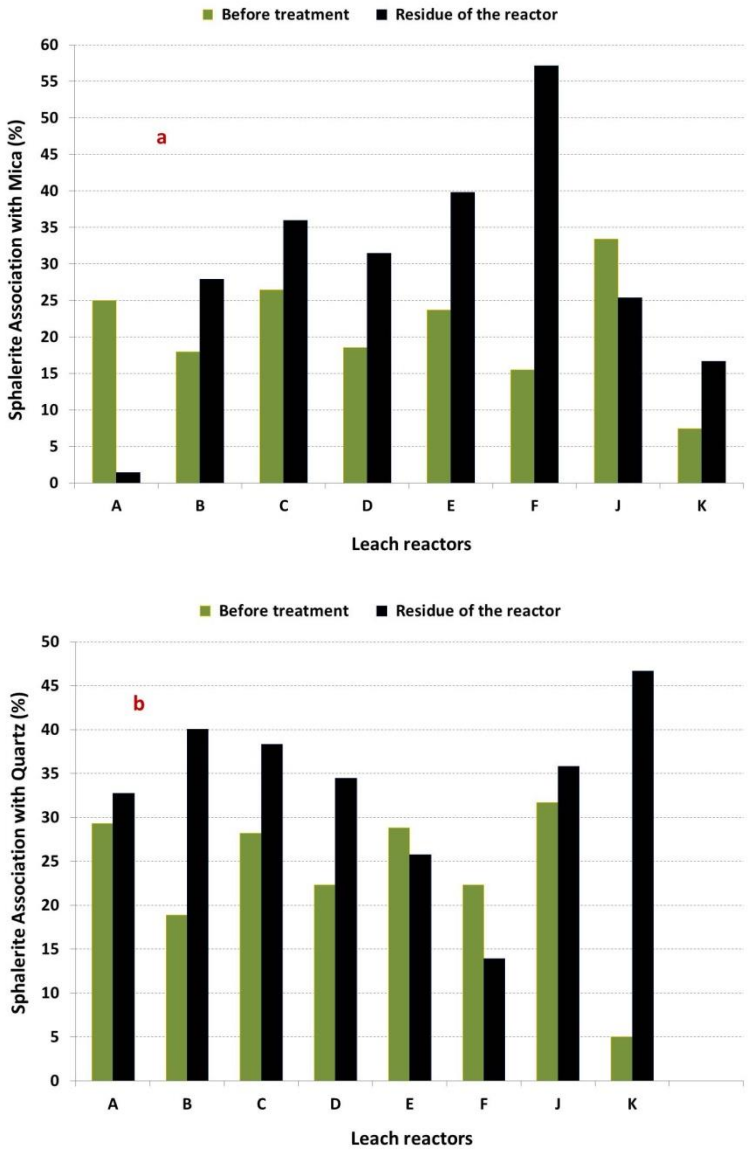

Figure 7: QEMSCAN® analysis results for the trend of the sphalerite association with Mica (a) and quartz (b) in the leach reactors before and after leaching process.

Effect of mineralogy on zinc extraction: Jarosite precipitation

Jarosite precipitation is an important phenomenon that is observed in many bacterial cultures. In the bacterial leaching of sulfide minerals, ferric iron is the key oxidizing agent and soluble iron species are the main determinants of redox potential. Active iron oxidizing bacteria, such as *Acidithiobacillus ferrooxidans* and *Leptospirillum ferrooxidans*, maintain high Fe^{3+}/Fe^{2+} ratios due to continued oxidation as part of their respiratory process. During bioleaching, monovalent cations (e.g., K^+ and Na^+) released from the alteration of silicate phases (e.g., Mica as a potassium aluminium silicate) present in the ore may promote the precipitation of ferric iron mainly as K-jarosite, which is controlled by pH (Ahonen and Tuovinen, 1995).

The limited extraction of metals has often been attributed to the formation of these secondary phases during bioleaching (Ahonen and Tuovinen, 1995; Harmer et al., 2007). Jarosite caused an obstruction to mineral-microbe contact by forming a mass transfer barrier to nutrients, oxygen, and carbon dioxide. Precipitation of iron hydroxide and jarosite phases in the leaching system may suppress the metal solubilisation by preventing contact between the leaching agent and the mineral. The solubility of iron species is defined by their concentration in solution and pH. Thus, the optimization of these parameters may greatly improve the metal recovery (Malik et al., 2004).

Jarosite precipitation during the leaching process was found to be minor. This would be as expected given the stable environment (stable redox potential and pH) in the leach reactors and the relatively low pH maintained. However, within the last month of leaching, evidence of precipitation was found. SEM images of selected samples in the Figure 8 show the progress of this phenomenon. EDS used for elemental analysis showed significant Fe, K, and S in the precipitation areas indicative of Fe (III)-hydroxysulfates. Table 5 shows the semi-quantitative elemental analysis of precipitation on the surface of ore particles (A, B and C crushed using HPGR at 95bars pressure setting), determined by EDS. It should be noted that elemental analysis of precipitation on the surface of ore particles in both cone crusher and HPGR products was same.

This was supported by the QXRD that showed the precipitation of Jarosite ($KFe_3(SO_4)_2(OH)_6$) up to 2 wt.% and Schwertmannite ($Fe_{16}O_{28}(SO_4)4H_{16}$) up to 5 wt.%. These minerals were not detected by QEMSCAN® most likely due to a combination of factors such as sample preparation, edge effect, soft texture, as well as the composition and discrimination of these phases from other ferric hydroxide species. A sulfide ore/concentrate should contain sufficiently high iron since the provision/availability of sufficient soluble iron in bioleaching environment is essential for the bacteria to generate ferric iron and efficiently drive the extraction of zinc from the complex sulfides

(Deveci *et a*l., 2004). The change in leaching from the readily accessible grains on the particle surface to the more inaccessible grains within particles is the main reason in this for precipitation.

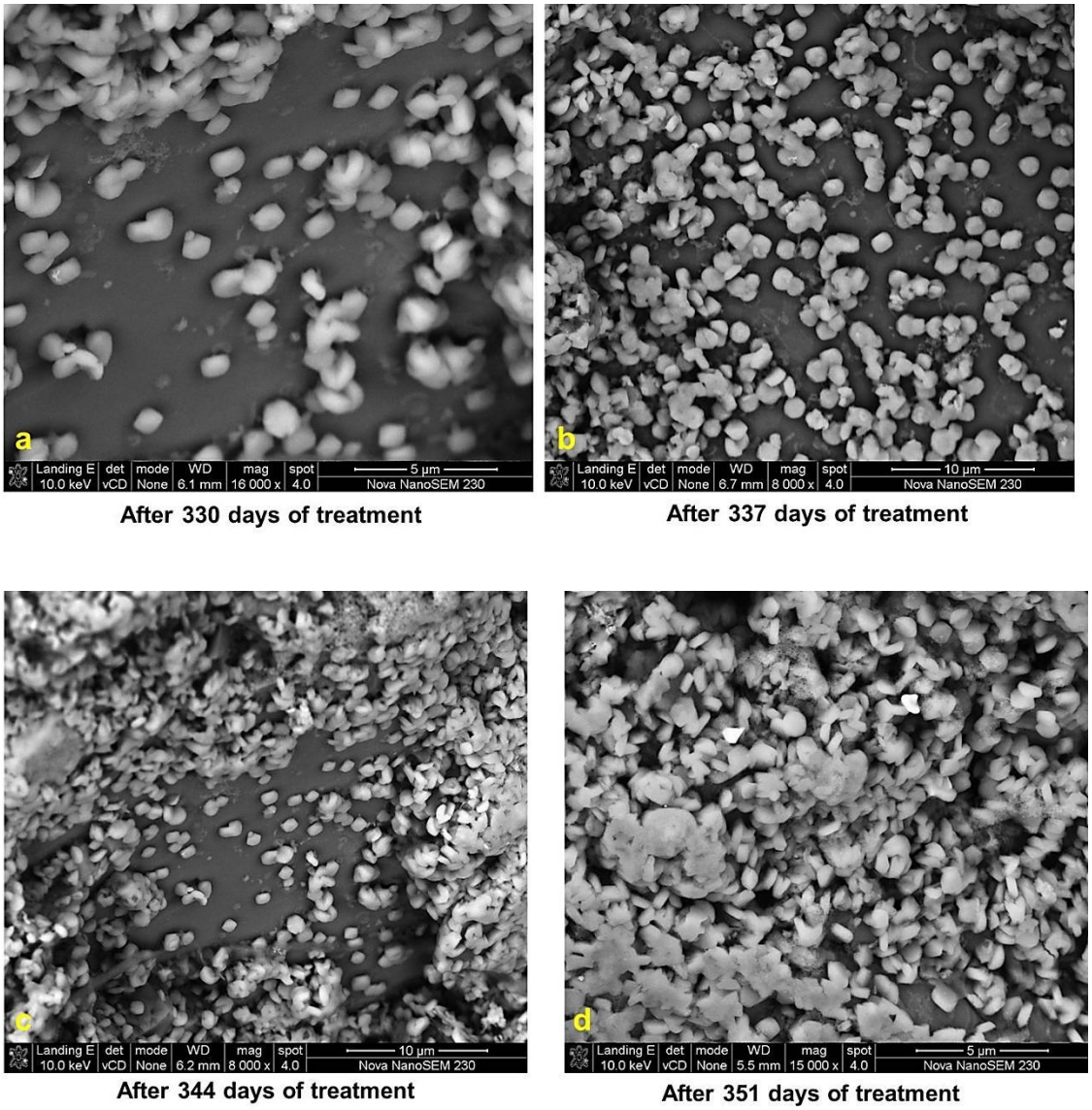

Figure 8: Growth trend of precipitation on the surface of particles from a to d.

During the leaching process, microorganisms regenerate ferric oxidant from the sufficient ferrous iron (Fe^{2+}) in the solution environment (1g/L in the media and dissolved from the ore). Slow oxidation rate of Zn during the last month of treatment in this study, affected balance of Fe^{2+} and Fe^{3+} ions concentration in the solution environment. High concentration of insoluble Fe^{3+}, due to the lack of demand precipitates as ferric hydroxide or precipitate as Fe(III)-hydroxysulfates such as

jarosites or schwertmannite. However, as there was no perceptible shift in solution potential at this time (Ghorbani et al., 2011e) it would be more likely that the leaching shifted from sphalerite to pyrite, thus causing a significant increase in the supply of Fe^{3+}.

Table 5: Semi-quantitative elemental analysis of the precipitate on the surface of ore particles (A, B and C crushed using HPGR at 95bars pressure setting) determined by EDS. (n.d. denotes not detected).

Element	Three different areas on the surface of the particles (wt. %)		
	A	B	C
O	> 20	> 20	> 20
Al	< 5	< 5	< 5
Si	10-20	10-20	10-20
S	5-10	< 5	< 5
K	< 5	< 5	< 5
Fe	< 5	< 5	< 5
Zn	n.d.	n.d.	n.d.

Effect of mineralogy on zinc extraction: Sphalerite composition

Characterization of the residue of the leach reactors indicated that there are areas within the ore particles where although sphalerite grains are accessible to the solution, they remain unreacted. Figure 9 shows unreacted sphalerite grains at the surface (Figure 9a) or in subsurface regions, which are accessible from the surface by cracks and pores (Figure 9b). These results indicate that accessibility to the reagent is necessary but not necessarily enough and a variety of mineralogical conditions can hamper or prevent leaching of an ore. Further investigations were done in these areas using EMPA to determine if the behaviour could be explained by any compositional variation or chemical zoning within the sphalerite.

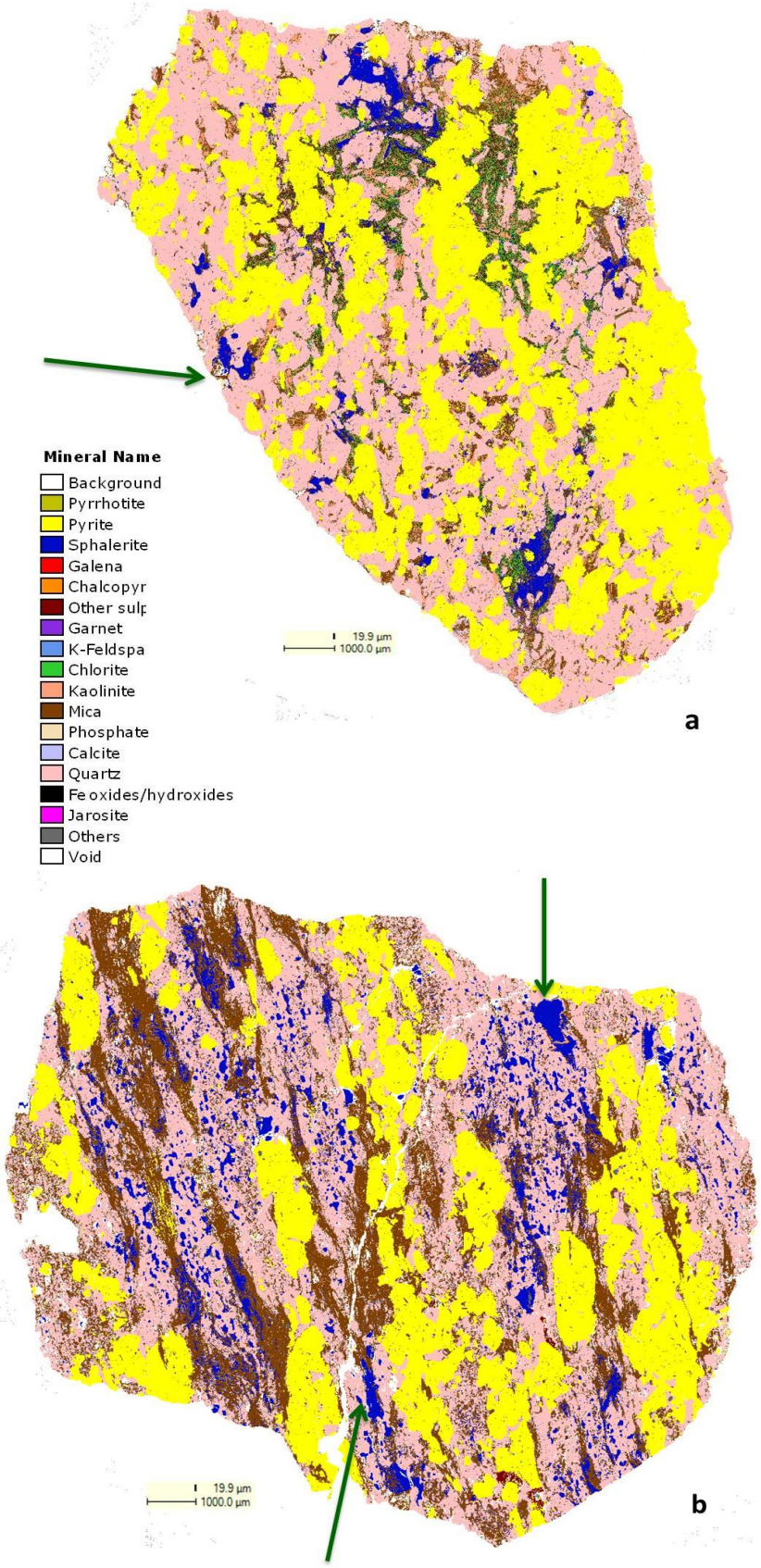

Figure 9: Unreacted sphalerite grains, at the surface (a) and subsurface accessible to the solution by crack (b).

Figures 10 and 11 show elemental maps of Zn, S, Fe, Mn and Cd and the accompanying QEMSCAN® images of unreacted sphalerite within the residue of particles prepared by HPGR (Figure 10) and cone crusher (Figure 11). The QEMSCAN® images of particles prepared by HPGR (small size fraction) have sphalerite with an associated void, most likely due to the prior dissolution of sphalerite. In contrast, particles prepared by cone crusher do not show this feature, which is consistent with the lower final zinc extraction.

Elemental maps show little true compositional variation within individual sphalerite grains. Associated spot analyses show that after eleven months of leaching treatment, sphalerite composition remains the same as the feed (see table 3). This shows a homogeneous and impervious environment within individual sphalerite grains. Sphalerite grains in the ore particles dissolve with varying size with constant density. During the leaching process, the radius gradually decreases with time, while the particle interior does not undergo much compositional change. In cases where the chemical reaction at the surface is much slower than the diffusion of reagents through the diffusion layer, the leaching becomes reaction controlled. This reaction trend in the mineral grain scale is in agreement with a shrinking sphere model.

Impurities within the sphalerite in the ore sample can also be rate-limiting factors in large particle leaching. Several previous studies (e.g. Morey *et al*., 2001; Harmer *et al*., 2007; Chen *et al*., 2010) have shown that variations in the mineral chemistry of sphalerite have a profound impact on its behaviour during processing. High levels of these impurities in some zinc concentrates, such as those produced at Gamsberg zinc mine, may render them unsuitable for processing by traditional Roast-Leach-Electrowinning (RLE) operations (McClung and Viljoen, 2011; Schouwstra *et al*., 2010). Therefore, the effect of the significant Fe and Mn contamination of sphalerite in this study needs evaluation. Although there is little Fe and Mn compositional variation within this sphalerite, it is compositionally quite different to pure ZnS and so the effects described in the following are considered significant.

It is well known that Fe influences both the sphalerite band gap and reactivity (Harmer *et al*., 2007). The result of study by Weisener *et al*. (2004) showed that the greater the concentration of Fe in the sphalerite, the greater the surface concentration of oxidised sulfur species observed. It appears likely that the elemental sulphur formed remains highly porous thus allowing the reactants and products to diffuse through or between the localised regions without significant diffusion control. The activation energies are consistent with a solid diffusion-controlled leach reaction rate. The activation energies for both Zn and Fe dissolution are dependent on the sphalerite Fe concentration and

decrease with increasing Fe concentration (Harmer *et al*., 2007; Weisener *et al*., 2004). This could be due to the availability of ferrous ions for ferric ion oxidation, which would increase the oxidation of zinc. This acceleration of the dissolution arising from the presence of Fe within the sphalerite could also be explained from the semiconduction and electrochemistry viewpoint. The iron content within sphalerite has the effect of narrowing the band gap energy, and consequently, the rate of dissolution of sphalerite is therefore directly proportional to the concentration of constitutional iron impurity in the solid. The iron content hence, formed a narrow impurity band within the forbidden band gap of the sphalerite, which energetically favoured the transfer of electron between the d-orbital band and the oxidant than the transfer of electrons between the valence band and the oxidant. Since sphalerite occurs as ferrous sphalerite, when iron substitutes for zinc, sphalerite dissolution generates acid instead of being acid consuming, due to hydrolysis of the ferric phases (Harmer *et al*., 2007, Schouwstra *et al*., 2010).

Although the elemental maps of sphalerite show little compositional variation in Mn, the presence of Mn within the ore in sphalerite, discrete FeMn silicates (pyroxmangite), Mn garnet (spessartine and almandine) and alabandite (MnS) would be associated with higher order oxidation products that may form refractory compounds of zinc and manganese. This could be a possible reason for unreacted sphalerite grains at the surface of the particle in the Figures 10 and 11, but further investigation need to be done with different type of sphalerite ore sample(s).

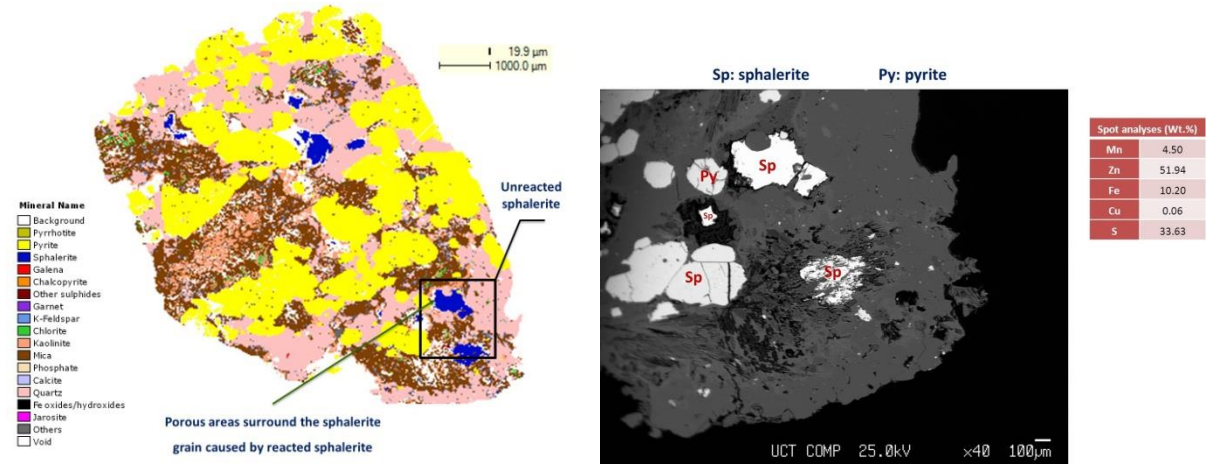

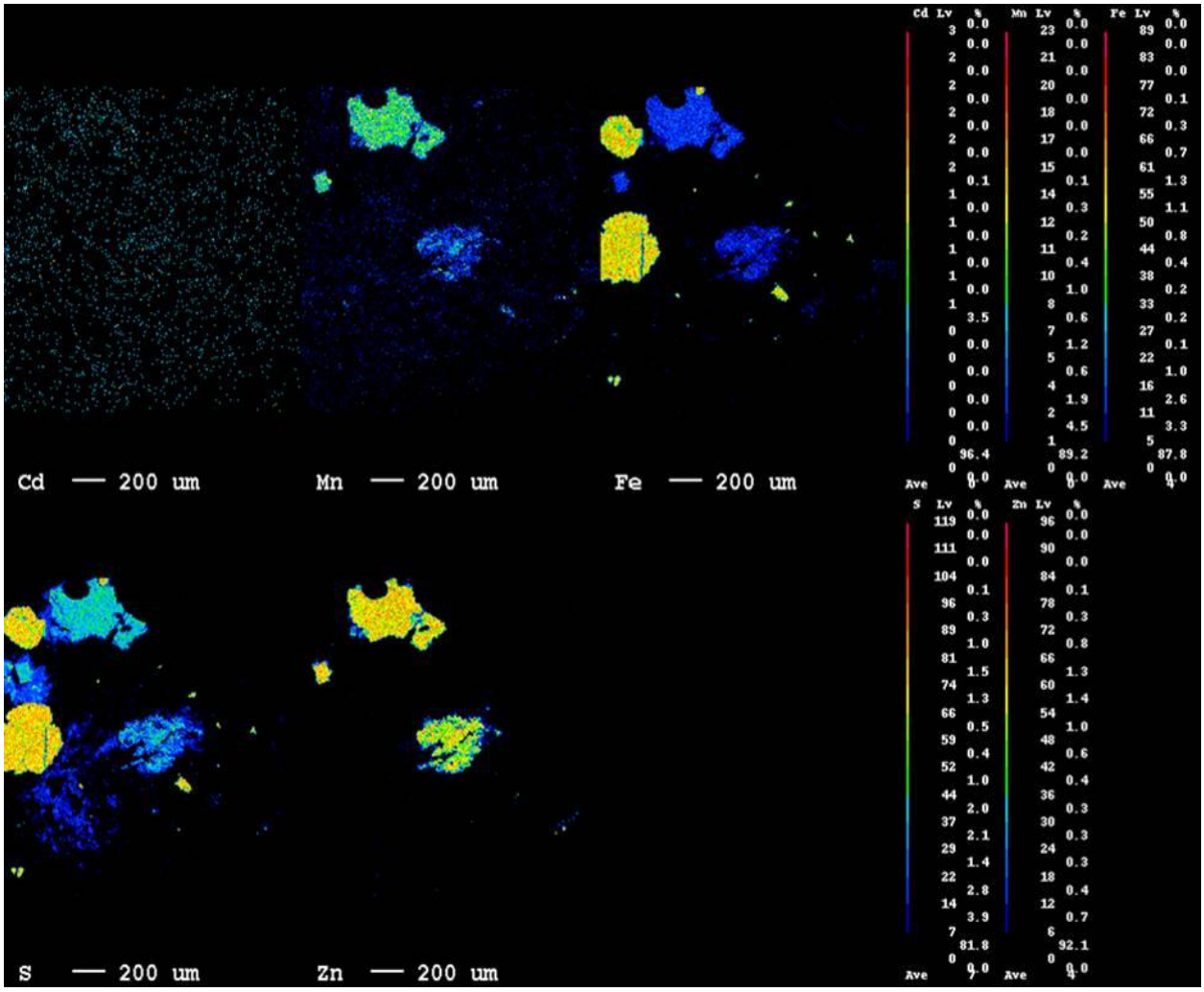

Figure 10: Back-scattered electron (BSE) and EMPA of elemental mapping for an area of the HPGR product from the leach reactor A (HPGR-95bar-small size fraction).

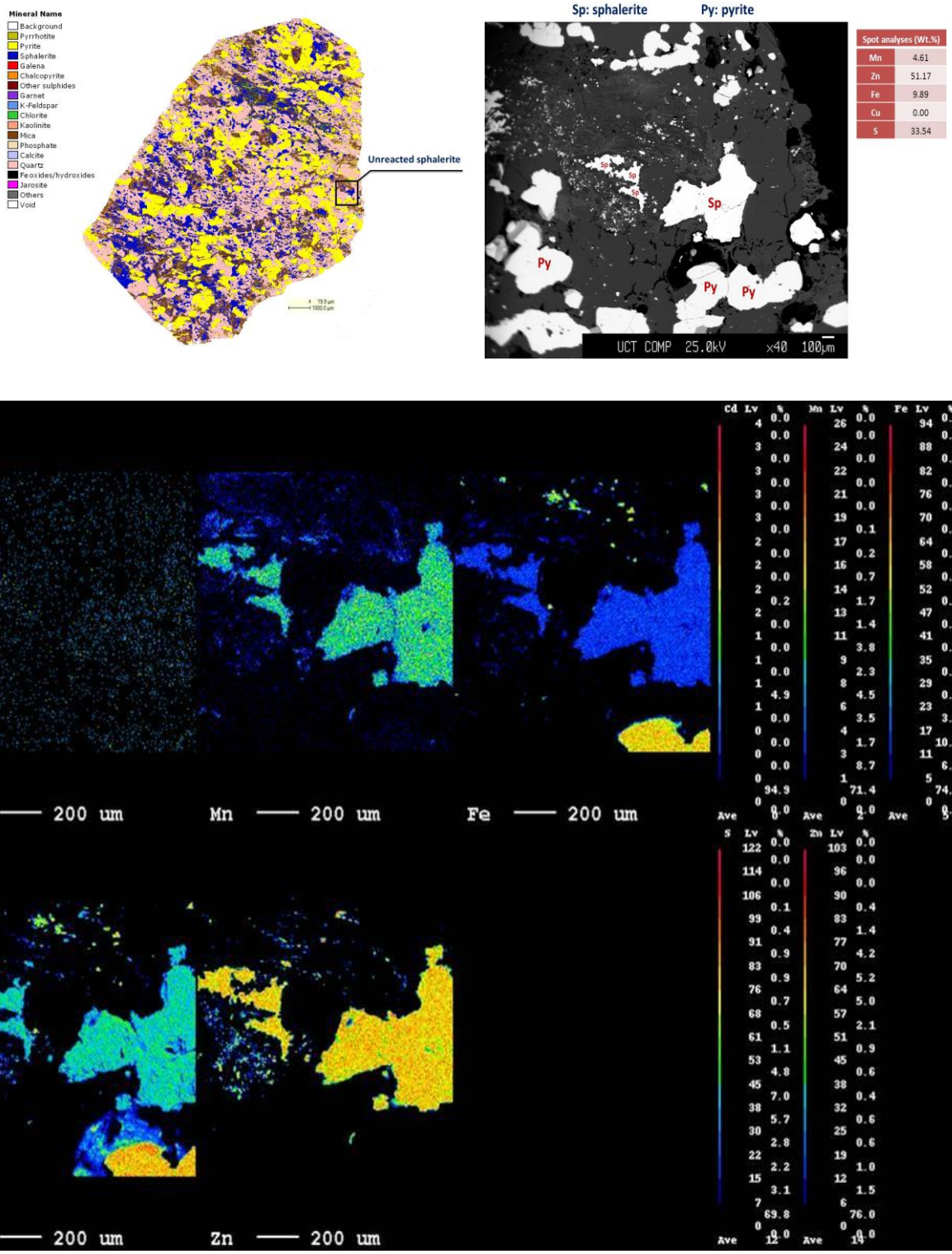

Figure 11: Back-scattered electron (BSE) and EMPA of elemental mapping for an area of the cone crusher product from the leach reactor J (cone crusher-large size fraction).

CONCLUSION

In this study, the role of mineralogy as a rate-limiting factor in large particle leaching was investigated using 3D particle characterisation from X-ray CT in combination with detailed 2D mineralogical characterisation (QEMSCAN®, EMPA, SEM/EDS). The most specific focus was on the effect of mineral chemistry and impurity content, mineral association and mineral precipitation on the rate of sphalerite leaching.

Characterization of the residue of the leach reactors indicated that there are areas within the ore particles where although sphalerite grains are accessible to the solution, they remain unreacted.

X-ray tomography and QEMSCAN® analysis of the selected samples before, during and after leaching, showed that the effect of galvanic interaction increases the leaching of the sphalerite grains that were associated to pyrite. Investigation also indicated that coatings on sphalerite grains due to the mica alteration cover the mineral surface from the solution-mineral interaction. The mineral chemistry was also measured to investigate the effect of the impurity content (Fe, Mn) on the rate of sphalerite leaching.

These results indicate that although accessibility to the reagent is necessary, a variety of the mineralogical conditions can hamper or prevent leaching of an ore. The systematic investigation need to be done on the characterization of the ore sample before starting any treatment on the ore.

ACKNOWLEDGEMENTS

The authors are grateful to Dr Kirsten Corin for the QXRD analysis; Prof. Dave Reid (Department of Geological Science, UCT), Paul Keanly (X-Sight X-ray Services), and the Centre for Advanced Scanning Technologies (Department of Physics, UCT) for their advice and support. Financial support from the South Africa Research Chair Initiative (SARChI) in Mineral Beneficiation, and a Research Niche Area (RNA) grant from the National Research Foundation (NRF) of South Africa are also acknowledged.

REFERENCES

Acevedo, F., 2002, Present and future of bioleaching in developing countries. Electronic Journal of Biotechnology, 52-56.

Ahonen, L., Tuovinen, O. H., 1995, Bacterial leaching of complex sulfide ore samples in bench-scale column reactors. Hydrometallurgy, 37, 22-36.

Arce, E. M., González, I., 2002, A comparative study of electrochemical behaviour of chalcopyrite, chalcocite and bornite in sulphuric acid solution, Int. J. Miner. Process, 67, 17-28.

Barton, P. B., Bethke P. M., 1987, Chalcopyrite disease in sphalerite: Pathology and epidemiology, American Mineralogist, 72, 451-467.

Bhatti, T.M., Bigham, J. M., Vuorinen, A., Tuovinen, O. H., 2011, Weathering of phlogopite in simulated bioleaching solutions, International Journal of Mineral Processing, 98, 30-34

Bhatti, T.M., Bigham, J. M., Vuorinen, A., Tuovinen, O. H., 2012, Chemical and bacterial leaching of metals from black schist sulfide minerals in shake flasks, International Journal of Mineral Processing, 110-111, 25-29.

Bigham, J. M., Bhatti, T.M., Vuorinen, A., Tuovinen, O. H., 2001, Dissolution and structural alteration of phlogopite mediated by proton attack and bacterial oxidation of ferrous iron, Hydrometallurgy , 59, 301-309.

Chen, J.H., Chen, Y., LI, Y. G., 2010, Effect of vacancy defects on electronic properties and activation of sphalerite (110) surface by first-principles, Trans. Nonferrous Met. Soc. China, 20, 502-506.

Cruz, R., Luna-Sánchez, R.M., Lapidus, G.T., González, I., Monroy, M., 2005, An experimental strategy to determine galvanic interactions affecting the reactivity of sulfide mineral concentrates, Hydrometallurgy, 78, 198-208.

Deveci, H., Akcil, A. and Alp, I., 2004, Bioleaching of complex zinc sulfides using mesophilic and thermophilic bacteria: comparative importance of pH and iron, Hydrometallurgy, 73, 293-310.

Dreisinger, D., 2006, Copper leaching from primary sulfides: Options for biological and chemical extraction of copper, Hydrometallurgy, 83, 10-21.

Ghorbani, Y., Becker, M., Mainza, M., Franzidis, J-P., Petersen, J., 2011a, Large particle effects in chemical/biochemical heap leach processes-A review, Minerals Engineering 24, 1172-1184.

Ghorbani, Y., Petersen, J., Becker, M., Mainza, A., Franzidis, J-P., 2011b, Investigation of heap leaching at the particle scale using X-ray computed tomography, International Conference on Percolation leaching: The status globally and in southern Africa, 8-9 November, Misty Hills, Muldersdrift, South Africa, 221-236.

Ghorbani, Y., Mainza, A.N., Petersen, J., Becker, M., Franzidis, J-P., Kalala, J.T., 2012c, Investigation of particles with high crack density produced by HPGR and its effect on the redistribution of the particle size fraction, Minerals Engineering- DOI:10.1016/j.mineng.2012.08.010.

Ghorbani, Y., Becker, M., Petersen, J., Morar, S. H., Mainza, A., Franzidis, J-P., 2011d, Use of X-ray computed tomography to investigate crack distribution and mineral dissemination in sphalerite ore particles, Minerals Engineering 24, 1249-1257.

Ghorbani, Y., Petersen, J., Becker, M., Mainza, A.N., Franzidis, J-P., 2013e, Investigation and Modelling of the Progression of Zinc Leaching from Large Sphalerite Ore Particles, Hydrometallurgy, (131-132), 8-23.

Harmer, S.L., Goncharova, L.V., Kolarova, R., Lennard, W.N., Munoz-Marquez, M.A., Mitchell, I.V., Nesbitt, H.W., 2007, Surface structure of sphalerite studied by medium energy ion scattering and XPS , Surface Science, 601, 352-361.

Kocabag, D., 1985, The effect of grinding media and galvanic interactions upon the flotation of sulfide minerals. Complex Sulfides, Process Symposium, 5, pp. 81-97.

Leonard, R.A, Weed, S.B., 1970, Mica weathering rate as related to mica type and composition, Clays and Clay Minerals, 18, 187-195.

Liddell, K. C., 2005, Shrinking core models in hydrometallurgy: What students are not being told about the pseudo-steady approximation, Hydrometallurgy, 79, 62-72.

Liu, Q., Li, H., Zhou, L., 2008, Galvanic interactions between metal sulfide minerals in a flowing system: Implications for mines environmental restoration, Applied Geochemistry, 23, 2316-2323.

Malik, A., Dastidar, M. G. and Roychoudhury, P. K., 2004, Factors limiting bacterial iron oxidation in biodesulphurization system. International Journal of Mineral Processing, 73, 34-42.

Malmström, M. E., Berglund, S. and Jarsjö, J., 2008, Combined effects of spatially variable flow and mineralogy on the attenuation of acid mine drainage in groundwater, Applied Geochemistry, 23, 1419-1422.

McClung, C.R., Viljoen, F., 2011, A detailed mineralogical assessment of sphalerites from the Gamsberg zinc deposit, South Africa: The manganese conundrum, Minerals Engineering, 24, 930-938.

Mellado, M. E., Cisternas, L. A. and Gálvez, E. D., 2009, An analytical model approach to heap leaching. Hydrometallurgy, 95, 33-42.

Morey, M.S., Grano, S.R., Ralston, J., Prestidge,C.A., Verity,B., 2001, The electrochemistry of Pb activated sphalerite in relation to flotation, Minerals Engineering, 14, 1009-1017.

Rao, S.R., Finch, J.A., 1988, Galvanic interaction studies on sulphide minerals. Canadian Metallurgical Quarterly 27, 253-259.

Rawlings, D. E., Tributsch H. and Hansford, G. S., 1999, Reasons why 'Leptospirillum'-like species rather than Thiobacillus ferrooxidans are the dominant iron-oxidizing bacteria in many commercial processes for the biooxidation of pyrite and related ores, Microbiology, 145, 5-13.

Rawlings, D., 2005, Characteristics and adaptability of iron and sulphur-oxidising microorganisms used for the recovery of metals from minerals and their concentrates", Microbial Cell Factories, 4, 312-322.

Schouwstra, R., De Vaux, D., Hey, P., Malysiak, V., Shackleton, N., Bramdeo, N., 2010, Understanding Gamsberg-A geometallurgical study of a large stratiform zinc deposit , Minerals Engineering, 23, 960-967.

Spry, P. G., Petersen, E. U., 1989, Zincian högbomite as an exploration guide to metamorphosed massive sulphide deposits, Mineralogical Magazine, 53, 263-969.

Sracek, O., Gélinas, P., Lefebvre, R. and Nicholson, R. V., 2006, Comparison of methods for the estimation of pyrite oxidation rate in a waste rock pile at Mine Doyon site, Quebec, Canada. Journal of geochemical exploration, 91, 99-112.

Strömberg, B. and Banwart, S., 1999, Experimental study of acidity-consuming processes in mining waste rock: some influences of mineralogy and particle size. Applied Geochemistry, 14, 1-13.

Urbano, G., Meléndez, A.M., Reyes, V.E., Veloz, M.A. and González, I., 2007, Galvanic interactions between galena-sphalerite and their reactivity International Journal of Mineral Processing, 82, 148-159.

Veglio, F., Trifoni, M., Pagnanelli, F., Toro, L., 2001, Shrinking core model with variable activation energy: a kinetic model of manganiferous ore leaching with sulphuric acid and lactose. Hydrometallurgy 60 (2), 167-179.

Watling, H.R., 2006, The bioleaching of sulfide minerals with emphasis on copper sulfides-A review, Hydrometallurgy, 84, 81-102.

Weisener, C. G., Smart, R. St.C., Gerson, A. R., 2004, A comparison of the kinetics and mechanism of acid leaching of sphalerite containing low and high concentrations of iron, Int. J. Miner. Process, 74, 239-249.